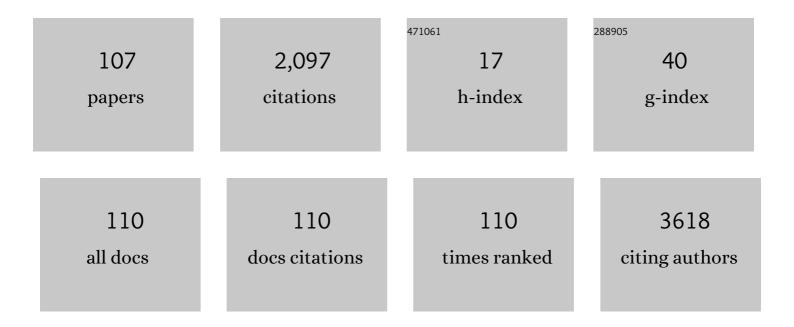
Alessandro Bevilacqua

List of Publications by Year in descending order

Source: https://exaly.com/author-pdf/8588172/publications.pdf Version: 2024-02-01



#	Article	IF	CITATIONS
1	3D tumor spheroid models for in vitro therapeutic screening: a systematic approach to enhance the biological relevance of data obtained. Scientific Reports, 2016, 6, 19103.	1.6	755
2	CIDRE: an illumination-correction method for optical microscopy. Nature Methods, 2015, 12, 404-406.	9.0	129
3	An SVM classifier to separate false signals from microcalcifications in digital mammograms. Physics in Medicine and Biology, 2001, 46, 1651-1663.	1.6	84
4	Cell Counting and Viability Assessment of 2D and 3D Cell Cultures: Expected Reliability of the Trypan Blue Assay. Biological Procedures Online, 2017, 19, 8.	1.4	70
5	People Tracking Using a Time-of-Flight Depth Sensor. , 2006, , .		59
6	Cancer multicellular spheroids: Volume assessment from a single 2D projection. Computer Methods and Programs in Biomedicine, 2015, 118, 95-106.	2.6	59
7	Human, All Too Human? An All-Around Appraisal of the "Artificial Intelligence Revolution―in Medical Imaging. Frontiers in Psychology, 2021, 12, 710982.	1.1	53
8	Multiâ€image based method to correct vignetting effect in light microscopy images. Journal of Microscopy, 2012, 248, 6-22.	0.8	44
9	High-Quality Real Time Motion Detection Using PTZ Cameras. , 2006, , .		35
10	Automated image mosaics by nonâ€ a utomated light microscopes: the <i>MicroMos</i> software tool. Journal of Microscopy, 2013, 252, 226-250.	0.8	29
11	An effective real-time mosaicing algorithm apt to detect motion through background subtraction using a PTZ camera. , 0, , .		28
12	Long term morphological characterization of mesenchymal stromal cells 3D spheroids built with a rapid method based on entry-level equipment. Cytotechnology, 2016, 68, 2479-2490.	0.7	26
13	Identification of Sclerostin as a Putative New Myokine Involved in the Muscle-to-Bone Crosstalk. Biomedicines, 2021, 9, 71.	1.4	26
14	Effects of Guided Random Sampling of TCCs on Blood Flow Values in CT Perfusion Studies of Lung Tumors. Academic Radiology, 2015, 22, 58-69.	1.3	24
15	Protein kinase B/AKT isoform 2 drives migration of human mesenchymal stem cells. International Journal of Oncology, 2013, 42, 118-126.	1.4	23
16	Extended depth of focus in optical microscopy: Assessment of existing methods and a new proposal. Microscopy Research and Technique, 2012, 75, 1582-1592.	1.2	22
17	A Fast and Reliable Image Mosaicing Technique with Application to Wide Area Motion Detection. Lecture Notes in Computer Science, 2007, , 501-512.	1.0	22

18 Real time detection of stopped vehicles in traffic scenes. , 2007, , .

#	Article	IF	CITATIONS
19	A new holistic 3D non-invasive analysis of cellular distribution and motility on fibroin-alginate microcarriers using light sheet fluorescent microscopy. PLoS ONE, 2017, 12, e0183336.	1.1	19
20	The Heterogeneity of Skewness in T2W-Based Radiomics Predicts the Response to Neoadjuvant Chemoradiotherapy in Locally Advanced Rectal Cancer. Diagnostics, 2021, 11, 795.	1.3	19
21	Single-image based methods used for non-invasive volume estimation of cancer spheroids: a practical assessing approach based on entry-level equipment. Computer Methods and Programs in Biomedicine, 2016, 135, 51-60.	2.6	18
22	TP53 drives abscopal effect by secretion of senescence-associated molecular signals in non-small cell lung cancer. Journal of Experimental and Clinical Cancer Research, 2021, 40, 89.	3.5	18
23	Quantitative Assessment of Effects of Motion Compensation for Liver and Lung Tumors in CT Perfusion. Academic Radiology, 2014, 21, 1416-1426.	1.3	17
24	Exploratory radiomic features from integrated 18F-fluorodeoxyglucose positron emission tomography/magnetic resonance imaging are associated with contemporaneous metastases in oesophageal/gastroesophageal cancer. European Journal of Nuclear Medicine and Molecular Imaging, 2019, 46, 1478-1484.	3.3	17
25	Automatically Extracted Machine Learning Features from Preoperative CT to Early Predict Microvascular Invasion in HCC: The Role of the Zone of Transition (ZOT). Cancers, 2022, 14, 1816.	1.7	17
26	Reproducibility of CT-based radiomic features against image resampling and perturbations for tumour and healthy kidney in renal cancer patients. Scientific Reports, 2021, 11, 11542.	1.6	16
27	Age-related skin analysis by capacitance images. , 2004, , .		15
28	Improving reliability of live/dead cell counting through automated image mosaicing. Computer Methods and Programs in Biomedicine, 2014, 117, 448-463.	2.6	15
29	A Methodological Approach to Parallel Simulated Annealing on an SMP System. Journal of Parallel and Distributed Computing, 2002, 62, 1548-1570.	2.7	14
30	ReViMS: Software tool for estimating the volumes of 3-D multicellular spheroids imaged using a light sheet fluorescence microscope. BioTechniques, 2017, 63, 227-229.	0.8	14
31	The Primacy of High B-Value 3T-DWI Radiomics in the Prediction of Clinically Significant Prostate Cancer. Diagnostics, 2021, 11, 739.	1.3	14
32	Joint Spatial and Tonal Mosaic Alignment for Motion Detection with PTZ Camera. Lecture Notes in Computer Science, 2006, , 764-775.	1.0	14
33	SYSTEM FOR AUTOMATIC DETECTION OF CLUSTERED MICROCALCIFICATIONS IN DIGITAL MAMMOGRAMS. International Journal of Modern Physics C, 2000, 11, 901-912.	0.8	13
34	A [68Ga]Ga-DOTANOC PET/CT Radiomic Model for Non-Invasive Prediction of Tumour Grade in Pancreatic Neuroendocrine Tumours. Diagnostics, 2021, 11, 870.	1.3	13
35	A High Performance Exact Histogram Specification Algorithm. , 2007, , .		12
36	Automatic detection of misleading blood flow values in CT perfusion studies of lung cancer. Biomedical Signal Processing and Control, 2016, 26, 109-116.	3.5	11

#	Article	IF	CITATIONS
37	CT Perfusion in Patients with Lung Cancer: Squamous Cell Carcinoma and Adenocarcinoma Show a Different Blood Flow. BioMed Research International, 2018, 2018, 1-10.	0.9	11
38	Vignetting correction by exploiting an optical microscopy image sequence. , 2011, 2011, 6166-9.		10
39	A novel approach for semi-quantitative assessment of reliability of blood flow values in DCE-CT perfusion. Biomedical Signal Processing and Control, 2017, 31, 257-264.	3.5	10
40	A 3-D Monte Carlo simulation of a small animal positron emission tomograph with millimeter spatial resolution. IEEE Transactions on Nuclear Science, 1999, 46, 697-701.	1.2	9
41	A dedicated system for breast cancer study with combined SPECT–CT modalities. Nuclear Instruments and Methods in Physics Research, Section A: Accelerators, Spectrometers, Detectors and Associated Equipment, 2003, 497, 129-134.	0.7	9
42	Optimizing parameters of a motion detection system by means of a distributed genetic algorithm. Image and Vision Computing, 2005, 23, 815-829.	2.7	9
43	Automatic Perspective Camera Calibration Based on an Incomplete Set of Chessboard Markers. , 2008, , .		9
44	Mosaicing of optical microscope imagery based on visual information. , 2011, 2011, 6162-5.		9
45	Illumination field estimation through background detection in optical microscopy. , 2011, , .		9
46	Reliable measurement of E. coli single cell fluorescence distribution using a standard microscope set-up. Journal of Biological Engineering, 2017, 11, 8.	2.0	9
47	A New Approach to Image Reconstruction in Positron Emission Tomography Using Artificial Neural Networks. International Journal of Modern Physics C, 1998, 09, 71-85.	0.8	8
48	OPTIMIZATION OF A DISTRIBUTED GENETIC ALGORITHM ON A CLUSTER OF WORKSTATIONS FOR THE DETECTION OF MICROCALCIFICATIONS. International Journal of Modern Physics C, 2001, 12, 55-70.	0.8	8
49	An incremental method for mosaicing of optical microscope imagery. , 2011, , .		8
50	A Distributed Genetic Algorithm for Parameters Optimization to Detect Microcalcifications in Digital Mammograms. Lecture Notes in Computer Science, 2001, , 278-287.	1.0	8
51	A novel approach to change detection based on a coarse-to-fine strategy. , 2005, , .		7
52	Vignetting and photo-bleaching correction in automated fluorescence microscopy from an array of overlapping images. , 2013, , .		7
53	Colour Vignetting Correction for Microscopy Image Mosaics Used for Quantitative Analyses. BioMed Research International, 2018, 2018, 1-15.	0.9	7
54	Liver CT perfusion: which is the relevant delay that reduces radiation dose and maintains diagnostic accuracy?. European Radiology, 2019, 29, 6550-6558.	2.3	7

#	Article	IF	CITATIONS
55	An efficient change detection algorithm based on a statistical non-parametric camera noise model. , 0, , .		6
56	EVALUATION OF A FULLY 3-D BPF METHOD FOR SMALL ANIMAL PET IMAGES ON MIMD ARCHITECTURES. International Journal of Modern Physics C, 1999, 10, 723-739.	0.8	6
57	A Simple Self-Calibration Method To Infer A Non-Parametric Model Of The Imaging System Noise. , 2005, , .		6
58	Occlusion Robust Vehicle Tracking based on SOM (Self-Organizing Map). , 2005, , .		6
59	Error analysis of satellite attitude determination using a vision-based approach. ISPRS Journal of Photogrammetry and Remote Sensing, 2013, 83, 19-29.	4.9	6
60	Semi-quantitative monitoring of confluence of adherent mesenchymal stromal cells on calcium-phosphate granules by using widefield microscopy images. Journal of Materials Science: Materials in Medicine, 2014, 25, 2395-2410.	1.7	6
61	Automatic classification of lung tumour heterogeneity according to a visual-based score system in dynamic contrast enhanced CT sequences. International Journal of Modern Physics C, 2016, 27, 1650106.	0.8	6
62	Advances in cancer modeling: fluidic systems for increasing representativeness of large 3D multicellular spheroids. BioTechniques, 2018, 65, 312-314.	0.8	6
63	A modular description for collimator geometry in EGS simulation tasks. , 0, , .		5
64	Coarse-to-fine strategy for robust and efficient change detectors. , 0, , .		5
65	A robust approach to reconstruct experimentally the camera response function. , 2008, , .		5
66	Parallel image restoration on parallel and distributed computers. Parallel Computing, 2000, 26, 495-506.	1.3	4
67	An effective multi-stage background generation algorithm. , 0, , .		4
68	In Vivo Quantitative Evaluation of Skin Ageing by Capacitance Image Analysis. , 2005, , .		4
69	Characterization of a capacitive imaging system for skin surface analysis. , 2008, , .		4
70	Real-time whole slide mosaicing for non-automated microscopes in histopathology analysis. Journal of Pathology Informatics, 2013, 4, 9.	0.8	4
71	Analysis of Beam-Induced Quenches of the LHC Cables With a Multi-Strand Model. IEEE Transactions on Applied Superconductivity, 2015, 25, 1-5.	1.1	4
72	Multislice Analysis of Blood Flow Values in CT Perfusion Studies of Lung Cancer. BioMed Research International, 2017, 2017, 1-11.	0.9	4

Alessandro Bevilacqua

#	Article	IF	CITATIONS
73	Open-Source Tools for Volume Estimation of 3D Multicellular Aggregates. Applied Sciences (Switzerland), 2019, 9, 1616.	1.3	4
74	SUV95th as a Reliable Alternative to SUVmax for Determining Renal Uptake in [68Ga] PSMA PET/CT. Molecular Imaging and Biology, 2020, 22, 1070-1077.	1.3	4
75	Density Distribution Maps: A Novel Tool for Subcellular Distribution Analysis and Quantitative Biomedical Imaging. Sensors, 2021, 21, 1009.	2.1	4
76	PREDICTING BIOLOGICAL AGE FROM A SKIN SURFACE CAPACITIVE ANALYSIS. International Journal of Modern Physics C, 2004, 15, 1309-1320.	0.8	3
77	An Automatic System for the Real-Time Characterization of Vehicle Headlamp Beams Exploiting Image Analysis. IEEE Transactions on Instrumentation and Measurement, 2010, 59, 2630-2638.	2.4	3
78	Manual Stage Acquisition and Interactive Display of Digital Slides in Histopathology. IEEE Journal of Biomedical and Health Informatics, 2014, 18, 1413-1422.	3.9	3
79	A novel algorithm to detect the baseline value of a time signal in Dynamic Contrast Enhanced-Computed Tomography. , 2018, , .		3
80	A Novel Vision-Based Approach for Autonomous Space Navigation Systems. Lecture Notes in Computer Science, 2009, , 837-846.	1.0	3
81	A 3-D Monte Carlo simulation of a small animal positron emission tomograph with millimeter spatial resolution. , 0, , .		2
82	EVALUATION OF SKIN AGEING THROUGH WRINKLE ANALYSIS IN CAPACITIVE IMAGES. International Journal of Modern Physics C, 2006, 17, 1663-1678.	0.8	2
83	Accurate eye-like segmentation in a heavily untextured contrasted scene. , 2008, , .		2
84	High accuracy estimation of vehicle trajectory using a real time stereo tracking system. , 2009, , .		2
85	An industrial vision-based technology system for the automatic test of vehicle beams. , 2009, , .		2
86	A CAPACITIVE IMAGE ANALYSIS SYSTEM TO CHARACTERIZE THE SKIN SURFACE. International Journal of Modern Physics C, 2009, 20, 2027-2041.	0.8	2
87	Computer assisted detection of regions of interest in histopathology using a hybrid supervised and unsupervised approach. Proceedings of SPIE, 2013, , .	0.8	2
88	Co-Density Distribution Maps for Advanced Molecule Colocalization and Co-Distribution Analysis. Sensors, 2021, 21, 6385.	2.1	2
89	An Image Registration Approach for Accurate Satellite Attitude Estimation. Lecture Notes in Computer Science, 2009, , 827-836.	1.0	2
90	A Single-Scan Algorithm for Connected Components Labelling in a Traffic Monitoring Application. Lecture Notes in Computer Science, 2003, , 677-684.	1.0	2

#	Article	IF	CITATIONS
91	Calibrating a Motion Detection System by Means of a Distributed Genetic Algorithm. , 0, , .		1
92	A vision-based approach for high accuracy assessment of satellite attitude. , 2009, , .		1
93	Analysis of CT Perfusion Blood Flow Maps in Patients with Lung Cancer: Correlation with the Overall Survival. , 2018, , .		1
94	Analysis of the effects of fitting errors of DCE-CT signals on perfusion parameters. , 2018, , .		1
95	Application of a plant phenotyping algorithm to detect stress caused by nematodes. Rhizosphere, 2018, 6, 86-88.	1.4	1
96	Modeling of Beam Loss Induced Quenches in the LHC Main Dipole Magnets. IEEE Transactions on Applied Superconductivity, 2019, 29, 1-7.	1.1	1
97	A Visual Perception Approach for Accurate Segmentation of Light Profiles. Lecture Notes in Computer Science, 2009, , 168-177.	1.0	1
98	Measuring Skin Topographic Structures through Capacitance Image Analysis. , 2006, , .		0
99	Image processing method for 3D volume rendering from one 2D projection: Application to Cancer spheroids. , 2014, , .		0
100	Image Processing Based Air Vehicles Classification for UAV Sense and Avoid Systems. , 2015, , .		0
101	Colormaps Of Computed Tomography Liver Perfusion Parameters Achieved Using Different Computing Methods Match. , 2019, , .		0
102	Texture Analysis of Non-Small Cell Lung Cancer on Unenhanced CT and Blood Flow Maps: a Potential Prognostic Tool. , 2019, , .		0
103	The effects of baseline length in Computed Tomography perfusion of liver. Biomedical Signal Processing and Control, 2020, 62, 102135.	3.5	0
104	Reproducibility of Computed Tomography perfusion parameters in hepatic multicentre study in patients with colorectal cancer. Biomedical Signal Processing and Control, 2021, 64, 102298.	3.5	0
105	Characterization of an FFDM unit based on a-Se direct conversion detector. , 2003, , 69-71.		0
106	High Quality-Speed Dilemma: A Comparison Between Segmentation Methods for Traffic Monitoring Applications. Lecture Notes in Computer Science, 2004, , 481-488.	1.0	0
107	A Simulation Framework to Assess Pattern Matching Algorithms in a Space Mission. Lecture Notes in Computer Science, 2011, , 404-413.	1.0	0